Electronic Supplementary Material (ESI) for Lab on a Chip.

Out-of-Equilibrium Biomolecular Interactions Monitored with Picosecond Fluorescence in Microfluidic Droplets
Supplementary Information

Sacha Maillot, Alain Carvalho, Jean-Pierre Vola, Christian Boudier, Yves Mély, Stefan Haacke, and Jérémie Léonard

1 Equilibrium measurements

A solution of Patent Blue Violet (PBV) and a solution of a mixture of PBV and Bovine Serum Albumine (BSA), both in Phosphate Buffered Saline (pH = 7.4) were circulated in a cuvette and their fluorescence decay measured with the streak camera. The results for [PBV] = 77 μM and [BSA] = 250 μM are shown in figure 1. The fluorescence kinetics of PBV could not be resolved with the streak camera which has a ∼10-ps (FWHM) wide Instrument Response Function (IRF). The signal of the complex with BSA is more than 8 times more intense and, more importantly, shows a significantly longer fluorescence lifetime.

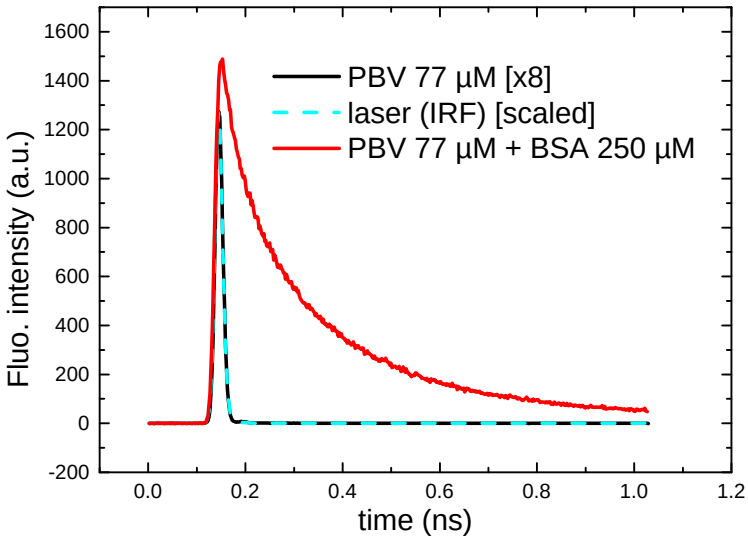

Figure 1: The fluorescence kinetics of PBV (black line) is not resolved and thus overlaps with the IRF (blue dashed line). The signal of the complex with BSA is shown in red.

2 Measurement of the droplet flow speed

The droplets flow speed is measured as follows. A white LED panel (Phlox SA) driven by a function generator (DS340, Stanford Research Systems), is used to shine the microfluidic chip with two 10-μs-short light pulses separated by a precisely defined time interval. The transmission of this double pulse by the microfluidic chip is recorded by a conventional CCD camera (C8484, Hamamatsu) in a single image acquisition via a removable mirror after the dichroic mirror shown in Fig. 1. The result, depicted in Fig. 2, is the superposition of two pictures separated in time by a known delay. The displacement of individual droplets during that delay time is measured to infer the droplet speed, which is in turn used to calibrate the correspondence between propagation length and relaxation time along the microfluidic channel.

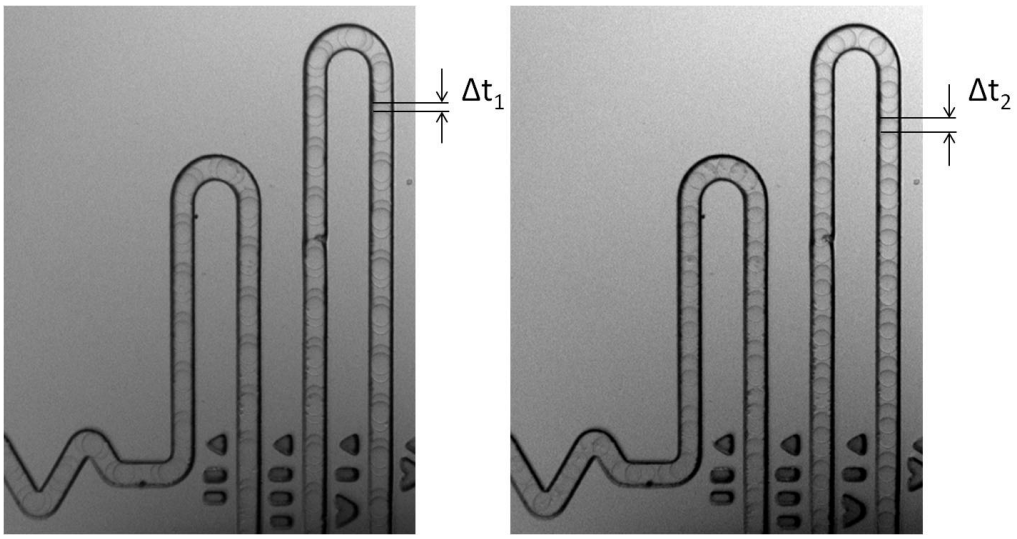

Figure 2: Droplets flowing in a 50 μm $\times$ 50 μm channel at 25 mm/s. The time interval between both light pulses is 1 ms (left) or 1.5 ms (right).

3 Quantitative data analysis

3.1 Fitting function

A fluorescence kinetics $F(t)$ can be fitted by a discrete sum of exponential decaying functions (amplitudes A_i, time constants τ_i), convoluted by the instrument response function (IRF) $R(t-t_0)$, with t_0 the time origin:

$$F(t) = \left\{ C + H(t) \times \left(\sum_i A_i e^{-t/\tau_i} \right) \right\} \otimes R(t-t_0). \tag{1}$$

Here C is a constant offset (determined at negative times) and $H(t)$ is the Heaviside function ($H(t) = 0$ for $t < 0$; $H(t) = 1$ for $t \geq 0$), which accounts for the fact that there is no signal before the initial excitation by a pulse of light.

Let us assume that $R(t)$ is a normalized gaussian function of standard deviation σ:

$$R(t) = \frac{1}{\sigma\sqrt{2\pi}} \exp\left(-\frac{t^2}{2\sigma^2}\right),$$

then the convolution can be analytically derived, using the error function, erf(t) :

$$\mathrm{erf}(t) = \frac{2}{\sqrt{\pi}} \int_0^t e^{-u^2} \,\mathrm{d}u.$$

Indeed the convolution reads:

$$F(t) = C + \frac{1}{\sigma\sqrt{2\pi}} \int_{-\infty}^{+\infty} H(t') \sum_i A_i \exp\left(-\frac{t'}{\tau_i}\right) \exp\left(-\frac{(t-t_0-t')^2}{2\sigma^2}\right) \mathrm{d}t'. \tag{2}$$

The argument of the exponential functions can be rewritten for each i:

$$-\frac{t'}{\tau_i} - \frac{(t-t_0-t')^2}{2\sigma^2} \;=\; -\frac{(t-t_0-\sigma^2/\tau_i-t')^2}{2\sigma^2} - \frac{t-t_0}{\tau_i} + \frac{\sigma^2}{2\tau_i^2}.$$

By operating the substitution $X = t' - (t - t_0 - \sigma^2/\tau_i)$, the convolution (2) reads:

$$F(t) = C \;+\; \frac{1}{\sigma\sqrt{2\pi}} \sum_i A_i \, e^{\frac{\sigma^2}{2\tau_i^2}} \, e^{-\frac{t-t_0}{\tau_i}} \int_{-\infty}^{+\infty} H(X + (t-t_0-\sigma^2/\tau_i)) \exp\left(-\frac{X^2}{2\sigma^2}\right) \mathrm{d}X.$$

which finally yields

$$\boxed{F(t) = C + \sum_i \left\{ \frac{A_i}{2} \exp\left(\frac{\sigma^2}{2\tau_i^2}\right) \exp\left(-\frac{t-t_0}{\tau_i}\right) \times \left[1 + \mathrm{erf}\left(\frac{t-t_0-\sigma^2/\tau_i}{\sigma\sqrt{2}}\right)\right] \right\}.} \quad (3)$$

Now we focus on the case where one fluorescence decay component τ is much shorter than the time resolution σ: $\tau \ll \sigma$. In the convolution (2), the exponential decaying function takes non vanishing values over an interval of a few τ's around $t' = 0$ (or $t' = \tau$). On that interval, the IRF varies very little and may be approximated by its Taylor development:

$$\begin{aligned} \text{with } f(t') &= \exp\left(-\frac{(t-t_0-t')^2}{2\sigma^2}\right) \quad (4) \\ f(t') &= \exp\left(-\frac{(t-t_0)^2}{2\sigma^2}\right) \times \left(1 + \frac{t-t_0}{\sigma^2}t' + \dots\right) \end{aligned}$$

Hence, one may write the convolution for this component in the following way:

$$\frac{1}{\sigma\sqrt{2\pi}} \int_{-\infty}^{+\infty} H(t')\ A \exp\left(-\frac{t'}{\tau}\right) \exp\left(-\frac{(t-t_0-t')^2}{2\sigma^2}\right) \mathrm{d}t' \quad (5)$$

$$= \frac{A}{\sigma\sqrt{2\pi}} \exp\left(-\frac{(t-t_0)^2}{2\sigma^2}\right) \int_0^{+\infty} \exp\left(-\frac{t'}{\tau}\right) \left(1 + \frac{t-t_0}{\sigma^2}t' + \cdots\right) \mathrm{d}t' \quad (6)$$

At the zeroth order of the Taylor expansion, the convolution reads:

$$A\,\tau \times \frac{1}{\sigma\sqrt{2\pi}} \exp\left(-\frac{(t-t_0)^2}{2\sigma^2}\right), \quad (7)$$

the IRF is simply multiplied by the integral $A \times \tau$ of the non resolved component.

Therefore, the explicit fitting function used in this work is thus given by $F(t)$ as defined by equation (3) for the time-resolved components, plus $A_0\,\tau_0$ multiplied by the IRF to account for putative non-resolved components:

$$\boxed{S(t) = A_0\,\tau_0 \frac{1}{\sigma\sqrt{2\,\pi}} \exp\left(-\frac{(t-t_0)^2}{2\sigma^2}\right) + F(t)} \quad (8)$$

Here we note that only the product $A_0\,\tau_0$ may be introduced as a fitting parameter and inferred from the fitting, while both individual parameters A_0 and τ_0 remain undetermined.

3.2 Global analysis

Global analysis is commonly applied to 2D datasets such as those obtained by spectrally- and time- resolved spectroscopy experiments (fluorescence or transient absorption). Here we follow the same lines with a 2D dataset being a chemical-time- and fluorescence-time-resolved signal, sometimes referred to as double-kinetic experiments.

SVD. The 40 fluorescence kinetics traces are gathered into a matrix $M_{ij} = F(T_i, t_j)$ whose horizontal dimension i represents the (millisec. to sec.) chemical relaxation time T_i and vertical dimension j represents the picosecond fluorescence kinetics time t_j at each time T_i of the chemical relaxation. A Singular Value Decomposition (SVD) algorithm is applied (Scilab software) to M_{ij} for data reduction and noise filtering. The SVD is a mathematical decomposition of the original M_{ij} matrix in the form:

$$M_{ij} = \sum_{mn} \chi_{im} S_{mn} F_{nj} = \sum_{n} \chi_n(T_i) s_n F_n(t_j) \tag{9}$$

In this decomposition, $S_{mn} = \delta_{mn} s_n$ is a diagonal matrix composed of the (sorted) singular values s_n. The columns of the χ_{im} matrix represent a set of $m = n$ "singular" chemical relaxation kinetics $\{\chi_n(T_i)\}$ associated to each of the n singular values. Conversely, the lines of F_{nj} matrix represent a set of n "singular" fluorescence kinetic traces $\{F_n(t_j)\}$.

Data reduction and noise filtering is performed by reconstructing the data set using Equation 9 while limiting the sum over n to a few dominant singular values. Figure

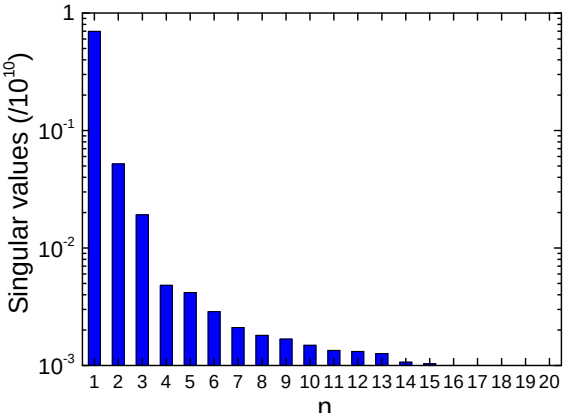

Figure 3: Singular values in logarithmic scale. The components $n > 3$ have a weight lower than 1% of the dominant component and are considered to contribute to the noise in the original dataset.

3 plots the singular values in the present case, and we restrict the data reconstruction to the first 3 singluar values. By doing so, only the singular fluorescence and chemical kinetics corresponding to the three dominant singular values are considered to contain relevant information while all the others are rejected as being noise. Figure 4 displays the three corresponding singular fluorescence kinetic traces weighted by their singular values $s_n F_n(t_j)$, for $n = 1$ to 3.

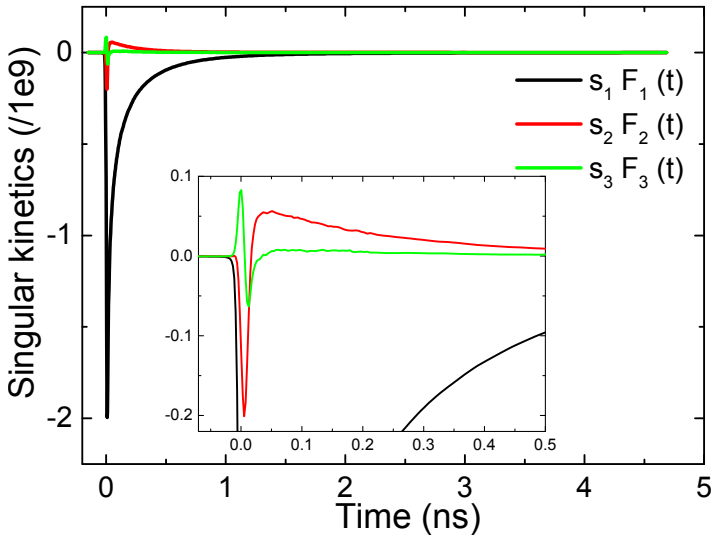

Figure 4: Singular kinetics $s_n F_n(t_j)$ for n=1,2 and 3. Inset: same graph zoomed in in the first 0.5 ns for qualitative comparison.

Global fitting is performed by fitting simultaneously the three dominant singular fluorescence kinetics $\{s_n F_n(t_j), n = 1..3\}$ by 3 fitting functions given by Eq. 8. By global fitting, we mean that we seek the same set of time constants $\{\tau_\alpha\}$ simultaneously in the three singular kinetics, while the corresponding amplitudes, as well as the non-resolved component $A_0\tau_0$ are left free to adjust differently in each of the three kinetics. Up to 4 time-resolved components $\tau_{1,...,4}$ should be included in the three fitting functions, to obtain satisfying residuals: the residuals are improved when fitting with 4 time-resolved components instead of 3, but not anymore with 5. Fig. 5 displays the results of this global fitting procedure for the three dominant singular fluorescence traces. To validate our choice of rejecting singular values for $n > 3$, we compare the residues obtained in the global fit to the singular fluorescence kinetics number 3 and 4 in Figure 6. The amplitudes of the residues are smaller than that of $s_3 F_3(t_j)$, but larger than that of $s_4 F_4(t_j)$, $s_5 F_5(t_j)$, etc..., justifying a posteriori the cutoff value of $n = 3$.

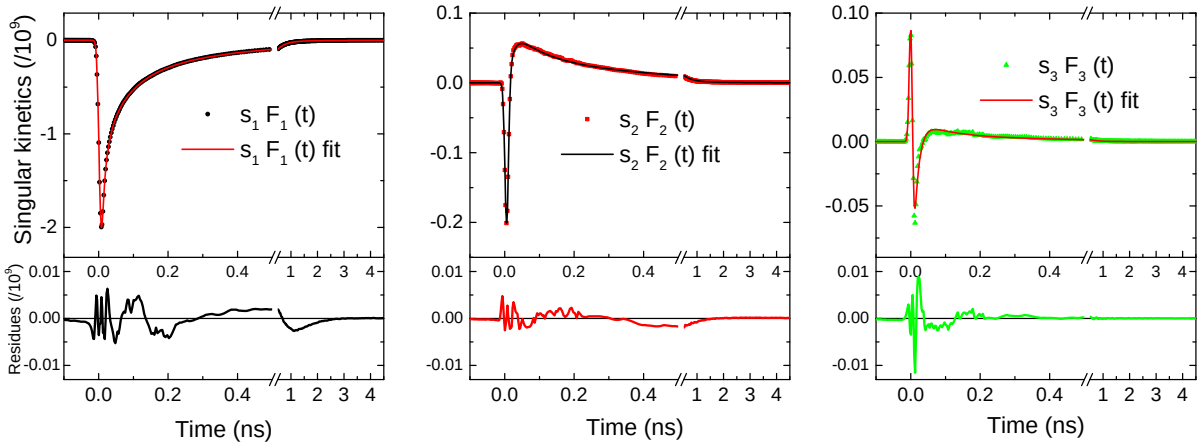

Figure 5: Results of the simultaneous fit of the three dominant singular fluorescence kinetics $s_1F_1(t_j)$, $s_2F_2(t_j)$ and $s_3F_3(t_j)$ by three functions (8) with 4 common time constants and a non-resolved component $A_0\tau_0$.

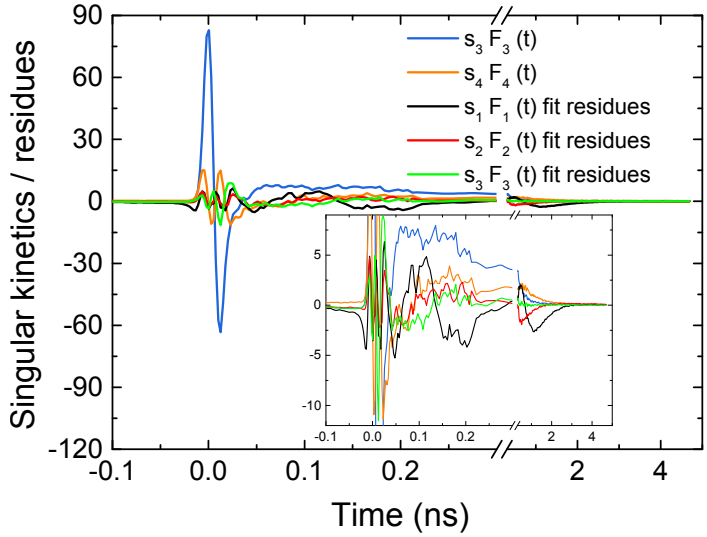

Figure 6: Residues of the simultaneous fit of the 3 dominant singular fluorescence kinetics compared to the singular kinetics $s_3F_3(t_j)$ and $s_4F_4(t_j)$. Insert: scaling for qualitative comparison. The amplitude of the residues is similar to that of the fourth singular kinetics: this confirms the choice of keeping the 3 first singular kinetics only.

The DARK's. The conclusion of the global fitting procedure consists in reconstructing the modelled data by applying Equation 9 to the three modelled singular fluorescence kinetics obtained by the simultaneous fit. Each of the three dominant kinetics was mod-

elled by a sum of exponentially decaying functions with a common set of time constants but individual sets of amplitudes:

$$\text{for } n = 1 \text{ to } 3: \quad s_n F_n(t_j) = \sum_{\alpha=0}^{4} A_{n\alpha} e^{-t_j/\tau_\alpha}.$$

Here for simplicity we disregard the convolution by the IRF and its consequence discussed above on whether each component is or not time resolved; this does not change the reasoning. We now use Eq. 9, to reconstruct the corresponding modelled data:

$$M_{ij} = \sum_{n=1}^{3} \chi_n(T_i) \times \sum_{\alpha=0}^{4} A_{n\alpha} e^{-t_j/\tau_\alpha} \tag{10}$$

$$= \sum_{\alpha=0}^{4} \left[\sum_{n=1}^{3} \chi_n(T_i) A_{n\alpha} \right] e^{-t_j/\tau_\alpha} \tag{11}$$

Hence we can define the Decay-Associated Reaction Kinetics DARK's:

$$\text{DARK}_\alpha(T_i) = \sum_{n=1}^{3} \chi_n(T_i) A_{n\alpha} \tag{12}$$

$$\text{and} \quad M_{ij} = \sum_{\alpha=0}^{4} \text{DARK}_\alpha(T_i) e^{-t_j/\tau_\alpha} \tag{13}$$

It thus appears that the DARK's represent the dependence with the chemical reaction time T_i of the amplitude of each exponential decaying function in the fluorescence decay kinetics measured along the structural relaxation of the bimolecular complex. We notice here that this overall global analysis leads to a model where T_i and t_j are separable variables: it may reproduce quantitatively well the data, but contains no physical input justifying such a separation between both variables.